CHEMISTRY OF MATERIALS
Article

Chem. Mater. **2011,** *23,* 1017–1022 1017
DOI:10.1021/cm103007v

Synthesis of Single-Crystalline Nanoplates by Spray Pyrolysis: A Metathesis Route to Bi_2WO_6

Amanda K. P. Mann and Sara E. Skrabalak*

Department of Chemistry, Indiana University, Bloomington, Indiana 47405, United States

Received October 19, 2010. Revised Manuscript Received December 6, 2010

Here, a solid-state metathesis reaction has been coupled with ultrasonic spray pyrolysis (USP) for the first time, yielding single-crystalline Bi_2WO_6 nanoplates. USP typically produces polycrystalline spherical particles, but by selecting precursors that yield Bi_2WO_6 and non-transient byproducts (e.g., NaCl), particles that are both single-crystalline and shape-controlled are achieved. This unprecedented result is directly correlated to the metathesis route employed to synthesize Bi_2WO_6 and contrasts with the results obtained when conventional precursors are used, which yields Bi_2WO_6 microspheres. Both the Bi_2WO_6 nanoplates and microspheres were extensively characterized. This comparative analysis found that the samples also differ in their surface terminations and hydrophilicity. Significantly, the integration of metathesis chemistry into spray pyrolysis may be generally applicable to the synthesis of a range of compositionally complex solids as single-crystalline samples.

Introduction

For the full potential of nanomaterials to be realized, scalable synthetic methods that yield solids with a well-defined size, shape, composition, and crystal-phase are required.[1,2] Given its simple experimental design and continuous nature, ultrasonic spray pyrolysis (USP) is an attractive method for the large-scale preparation of materials, but typically polycrystalline microspheres are produced.[3−5] This observation is the result of systematically selecting precursors that yield transient byproducts, which provide no templating or structure-directing effects during particle formation. Recently, porous and nanostructured particle architectures have been achieved by the incorporation or in situ generation of templates during USP.[6−18] However, particles that are both single-crystalline and shape-controlled have not been accessed previously. Yet, by integrating a solid-state metathesis reaction into USP, single-crystalline Bi_2WO_6 nanoplates are synthesized. Essential to their formation is the generation of a non-transient byproduct via the metathesis reaction. Otherwise, polycrystalline microspheres are produced. Significantly, such chemistry represents a new synthetic approach to generating non-transient byproducts during USP, which should provide a generally applicable means of controlling crystal growth during aerosol syntheses.

Owing to its interesting physical properties, Bi_2WO_6 was selected as an initial synthetic target to demonstrate the feasibility of coupling metathesis reactions with spray pyrolysis.[19−21] Bi_2WO_6 displays both piezoelectric and ferroelectric behavior, but most often it is studied for its photocatalytic properties, being a suitable visible-light photocatalyst for the degradation of dyes and organic pollutants and even the O_2-evolving half reaction for water splitting.[22−28] The conduction band of Bi_2WO_6

*To whom correspondence should be addressed. E-mail: sskrabal@indiana.edu.

(1) Xia, Y.; Xiong, Y. J.; Lim, B.; Skrabalak, S. E. *Angew. Chem., Int. Ed.* **2009**, *48*, 60.
(2) Kwon, S. G.; Hyeon, T. *Acc. Chem. Res.* **2008**, *41*, 1696.
(3) Kodas, T. T.; Hampden-Smith, M. *Aerosol Processing of Materials*; Wiley-VCH: New York, 1999.
(4) Messing, G. L.; Zhang, S. C.; Jayanthi, G. V. *J. Am. Ceram. Soc.* **1993**, *76*, 2707.
(5) Pratsinis, S. E. *Prog. Energy Combust. Sci.* **1998**, *24*, 197.
(6) Peterson, A. K.; Morgan, D. G.; Skrabalak, S. E. *Langmuir* **2010**, *26*, 8804.
(7) Suh, W. H.; Jang, A. R.; Suh, Y. H.; Suslick, K. S. *Adv. Mater.* **2006**, *18*, 1832.
(8) Skrabalak, S. E.; Suslick, K. S. *J. Am. Chem. Soc.* **2005**, *127*, 9990.
(9) Skrabalak, S. E.; Suslick, K. S. *J. Am. Chem. Soc.* **2006**, *128*, 12642.
(10) Fortunato, M. E.; Rostam-Abadi, M.; Suslick, K. S. *Chem. Mater.* **2010**, *22*, 1610.
(11) Lee, S. Y.; Gradon, L.; Janeczko, S.; Iskandar, F.; Okuyama, K. *ACS Nano* **2010**, *4*, 4717.
(12) Fan, H.; Van Swol, F.; Lu, Y.; Brinker, C. J. *J. Non-Cryst. Solids* **2001**, *285*, 71.
(13) Iskandar, F.; Mikrajuddin; Okuyama *Nano Lett.* **2001**, *1*, 231.
(14) Kim, S. H.; Liu, B. Y. H.; Zachariah, . R. *Chem. Mater.* **2002**, *14*, 2889.
(15) Lee, S. G.; Choi, S. M.; Lee, D. *Thermochim. Acta* **2007**, *455*, 138.
(16) Lu, Y.; Cao, G.; Kale, R. P.; Prabakar, S.; Lopez, G. P.; Brinker, C. J. *Chem. Mater.* **1999**, *11*, 1223.
(17) Lu, Y.; Fan, H.; Stump, A.; Ward, T. L.; Rieker, T.; Brinker, C. J. *Nature* **1999**, *398*, 223.
(18) Tsung, C.-K.; Nanfeng, J. F.; Shi, Z. Q.; Forman, A. J.; Wang, J.; Stucky, G. D. *Angew. Chem., Int. Ed.* **2008**, *47*, 8682.
(19) Wolfe, R. W.; Newnahm, R. E.; Kay, M. I. *Solid State Commun.* **1969**, *7*, 1797.
(20) Utkin, V. I.; Roginskaya, Y. E.; Voronkova, V. I.; Yanovskii, V. K.; Galyamov, B. S.; Venevtsev, Y. N. *Phys. Status Solidi A* **1980**, *59*, 75.
(21) Newkirk, H. W.; Liebertz, J.; Kockel, A.; Quadflie, P. *Ferroelectrics* **1972**, *4*, 51.
(22) Tang, J.; Zou, Z.; Ye, J. *Catal. Lett.* **2004**, *92*, 53.
(23) Fu, H.; Pan, C.; Yao, W.; Zhu, Y. *J. Phys. Chem. B* **2005**, *109*, 22432.
(24) Zhang, L.; Wang, W.; Chen, Z.; Zhou, L.; Xu, H.; Zhu, W. *J. Mater. Chem.* **2007**, *17*, 2526.
(25) Zhang, C.; Zhu, Y. *Chem. Mater.* **2005**, *17*, 3537.
(26) Amano, F.; Yamakata, A.; Nogami, K.; Osawa, M.; Ohtani, B. *J. Am. Chem. Soc.* **2008**, *130*, 17650.

Published on Web 01/10/2011

falls at +0.24 eV versus SHE, making it an unsuitable material for H_2 evolution, but complete water splitting may be achieved via composite formation.[29,30] Bi_2WO_6 is synthesized traditionally by solid state heating of Bi_2O_3 and WO_3, which results in low surface area powders with ill-defined features.[19,31] Yet, for many applications and especially studies of fundamental structure−function relationships, size- and shape-controlled samples are preferred.

Solvothermal,[23,26,32−34] electrospinning,[35,36] and sonochemical[37] routes to Bi_2WO_6 have been reported, often with hierarchical particle structures produced. Related to this article, Lee and co-workers recently reported the synthesis of Bi_2WO_6 microspheres by spray pyrolysis.[27] However, as reported here, the generation of non-transient byproducts can greatly alter the structure of Bi_2WO_6 particles prepared by USP, producing Bi_2WO_6 nanoplates. Their formation is attributed to the integration of metathesis chemistry into spray pyrolysis, with their mechanism of formation and properties being compared both to Bi_2WO_6 microspheres prepared by USP and samples from solid state heating of suitable precursors.

Experimental Section

Materials. All chemicals were handled in air and used as received. $BiCl_3$ (≥98%), $(NH_4)_{10}H_2(W_2O_7)_6$ (>99%), and Bi_2O_3 (99.9%) were purchased from Sigma Aldrich. $Bi(NO_3)_3 \cdot 5H_2O$ (98%), $BiBr_3$ (99%), Li_2WO_4 (99%), and $Na_2WO_4 \cdot 2H_2O$ (99%) were purchased from Alfa Aesar. WO_3 (99.9%) was purchased from Fluka. Deionized water was used in all syntheses.

Apparatus for Ultrasonic Spray Pyrolysis. A schematic of the laboratory-scale USP system used to prepare Bi_2WO_6 is shown in Supporting Information, Figure S1 and described fully in the Supporting Information. An ultrasonic transducer (1.7 MHz, ~5 W/cm^2) was used to nebulize the precursor solutions. An inert gas (N_2 99.0%, 55 sccm) served as a carrier through a heated tube furnace, with product particles being collected in water. Products were isolated by centrifugation (3900 rpms) and washed twice with water.

Synthesis of Bi_2WO_6 Microspheres (USP Bi_2WO_6). Fifteen milliliters of water was added to a vial containing 0.14 g of $(NH_4)_{10}H_2(W_2O_7)_6$ (0.000047 mol) and 0.372 g of $Bi(NO_3)_3$ (0.00075 mol). Upon the addition of water, the solution became white and opaque, indicating hydrolysis of $Bi(NO_3)_3$ and the formation of colloidal $BiONO_3$ and possibly basic bismuth nitrates (e.g., $[Bi_6O_5(OH)_3](NO_3)_5$).[38,39] To ensure full dispersion, the colloidal suspension was agitated in an ultrasonic bath (~1 min). The suspension was sparged with N_2 gas (99.0%) at 55 sccm for 30 min, followed by nebulization. The furnace temperature was 500 °C. Note: the Bi-to-W ratio in the precursor solution was adjusted to achieve stoichiometric Bi_2WO_6.

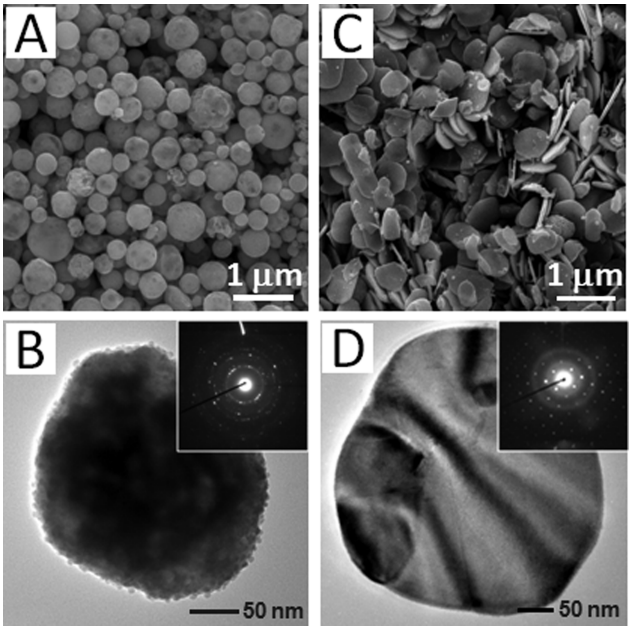

Figure 1. (A) SEM and (B) TEM images, inset ED, of Bi_2WO_6 microspheres (sample USP Bi_2WO_6). (C) SEM and (D) TEM images, inset ED, of Bi_2WO_6 nanoplates (sample USP-M Bi_2WO_6).

Synthesis of Bi_2WO_6 Nanoplates (USP-M Bi_2WO_6). Fifteen milliliters of water was added to a vial containing 0.25 g of $Na_2WO_4 \cdot 2H_2O$ (0.00075 mol) and 0.4726 g of $BiCl_3$ (0.0015 mol). Upon the addition of water, the solution became white and opaque, indicating hydrolysis of $BiCl_3$ and the formation of colloidal BiOCl.[40] To ensure full dispersion, the colloidal suspension was agitated in an ultrasonic bath (~1 min). The suspension was then sparged with N_2 gas (99.0%) at 55 sccm for 30 min, followed by nebulization. The furnace temperature was 600 °C.

Synthesis of Bi_2WO_6 from the Parent Oxides (SS Bi_2WO_6). Conventional Bi_2WO_6 was synthesized as reported by Kay et al.[19] A 0.5 g portion of WO_3 and 1.005 g of Bi_2O_3 were mixed and ground with a mortar and pestle for 2 min. The yellow-green powder was placed in a ceramic crucible and heated under static air for 24 h at 800 °C.

Synthesis of Bi_2WO_6 from Na_2WO_4 and $BiCl_3$ (SS-M Bi_2WO_6). Fifteen milliliters of water was added to 0.25 g of Na_2WO_4 (0.00075 mol) and 0.4726 g of $BiCl_3$ (0.0015 mol). To ensure full dispersion, the resulting suspension was agitated in an ultrasonic bath briefly. The suspension was then dried under vacuum, placed in a ceramic crucible, and heated under air for 1 h at 600 °C. The product was washed with water to extract the byproduct salt, and the powder dried under vacuum.

Product Characterization. Product structures were examined by scanning electron microscopy (SEM) on FEI Quanta 600 FEG operating at 30 kV. Energy dispersive X-ray spectroscopy (EDS) was performed with an Oxford Inca detector interfaced to the FEI Quanta 600 FEG at 30 kV without sample sputtering.

(27) Huang, Y.; Ai, Z.; Ho, W.; Chen, M.; Lee, S. *J. Phys. Chem. C* **2010**, *114*, 6342.
(28) Kudo, A.; Hijii, S. *Chem. Lett.* **1999**, *28*, 1103.
(29) Kitano, M.; Hara, M. *J. Mater. Chem.* **2010**, *20*, 627.
(30) Hu, C.-C.; Nian, J.-N.; Teng, H. *Sol. Energy Mater. Sol. Cells* **2008**, *92*, 1071.
(31) Rangel, R.; Bartolo-Pérez, P.; Gómez-Cortés, A.; Díaz, G.; Fuentes, S.; Galván, D. H. *J. Mater. Synth. Process.* **2001**, *9*, 207.
(32) Ma, D.; Huang, S.; Chen, W.; Hu, S.; Shi, F.; Fan, K. *J. Phys. Chem. C* **2009**, *113*, 4369.
(33) Ren, J.; Wang, W.; Sun, S.; Zhang, L.; Chang, J. *Appl. Catal., B* **2009**, *92*, 50.
(34) Xie, H.; Shen, D.; Wang, X.; Shen, G. *Mater. Chem. Phys.* **2007**, *103*, 334.
(35) Shang, M.; Wang, W.; Ren, J.; Sun, S.; Wang, L.; Zhang, L. *J. Mater. Chem.* **2009**, *19*, 6213.
(36) Shang, M.; Wang, W.; Zhang, L.; Sun, S.; Wang, L.; Zhou, L. *J. Phys. Chem. C* **2009**, *113*, 14727.
(37) Zhou, L.; Wang, W.; Zhang, L. *J. Mol. Catal. A: Chem.* **2007**, *268*, 195.
(38) Greenwood, N. N.; Earnshaw, A. *Chemistry of the Elements*, 1st ed.; Pergamon Press, Inc.: Elmsford, NY, 1984.
(39) Christensen, A. N.; Jensen, T. R.; Scarlett, N. V. Y.; Madsen, I. C.; Hanson, J. C.; Altomare, A. *Dalton Trans.* **2003**, 3278.
(40) Diemente, D. *J. Chem. Educ.* **1997**, *74*, 398.

Scheme 1. (A) USP Synthesis of Bi_2WO_6 Using Conventional Precursors; (B) USP Synthesis of Bi_2WO_6 Using Precursors Capable of Metathesis Chemistry

$$\textbf{(A)}\ 24\ BiONO_{3(colloidal)} + (NH_4)_{10}H_2(W_2O_7)_{6(aq)} \xrightarrow{\Delta,\ USP} 12\ Bi_2WO_{6(s)} + \text{gaseous byproducts (e.g., } NH_3 \text{ and } N_2O_5)$$

$$\textbf{(B)}\ 2\ BiOCl_{(colloidal)} + Na_2WO_{4(aq)} \xrightarrow{\Delta,\ USP} Bi_2WO_{6(s)} + 2\ NaCl_{(s)}$$

Transmission electron microscopy (TEM) and electron diffraction (ED) were done on a JEOL JEM-2200FS TEM operating at 300 kV. N_2 isotherms were obtained with a Micromeretics ASAP 2020 using standard techniques. 3-point Brunauer, Emmett, and Teller (BET) analysis was employed to obtain surface area measurements. The samples were vacuum degassed at 120 °C (ramp rate of 1 K/min.) for 12 h. Powder X-ray diffraction (XRD) was performed on a Scintag diffractometer with Cu Kα radiation. Elemental analysis was conducted using a Perkin-Elmer Sciex Elan DRCe ICP-MS. Differential scanning calorimetry (DSC) was performed on a Q10 TA DSC with a ramp rate of 5 °C/minute. Hermetic aluminum pans with a pinhole were used to facilitate the release of evolved gases under a N_2 atmosphere. Thermal gravimetric analysis (TGA) was performed on a Q5000 IR TA TGA with a ramp rate of 10 °C/minute under a N_2 atmosphere; platinum pans were employed. For both DSC and TGA, USP precursor solutions were prepared as described then vacuum-dried to remove water prior to analysis. X-ray photoelectron spectroscopy (XPS) was conducted on a Kratos Axis Ultra XPS.

Results and Discussion

Synthesis and Shape Control. USP uses ultrasound to nebulize a precursor solution into a fine mist. A gas then carries the droplets into a furnace, with solvent evaporation occurring at low to moderate temperatures and the dissolved species decomposing and/or reacting with one another at higher temperatures.[3] As multiple nucleation sites exist within any given droplet, polycrystalline spheres are produced, with their size being governed by the modified Lang Equation.[41] To produce compositionally complex materials such as Bi_2WO_6, precursors are typically selected so that upon pyrolysis only the desired product and small gaseous byproducts are generated, which are flushed out of the system by the carrier gas.[3] This selection systematically removes any structure-directing or pore-templating species from the reaction phase. Indeed, submicrometer spheres of Bi_2WO_6 (diameter: 386 ± 114 nm; sample USP Bi_2WO_6) are readily prepared using $Bi(NO_3)_3$ and $(NH_4)_{10}H_2(W_2O_7)_6$ as precursors. SEM and TEM images of the product particles are shown in Figures 1A and 1B, respectively. Electron diffraction (ED) highlights the polycrystalline nature of the particles (Figure 1B, inset), which are similar to those prepared by Lee and co-workers in which bismuth citrate ($BiC_6H_5O_7$) and tungstic acid (H_2WO_4) were used as precursors dissolved in concentrated ammonia solution.[27] In the case of USP Bi_2WO_6, a solution containing colloidal $BiONO_3$ and dissolved tungstate anions results when water is added to the precursor salts,[38]

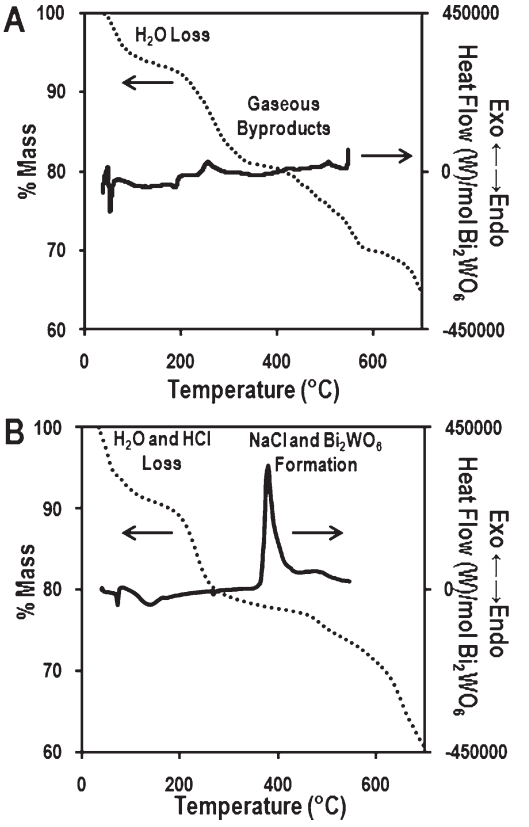

Figure 2. DSC (solid lines) and TGA (dotted lines) of the dried precursor combinations that produce (A) USP Bi_2WO_6 and (B) USP-M Bi_2WO_6. DSC scale is the right side ordinate axis; TGA is the left side ordinate axis.

which can be directly nebulized. In either case, pyrolysis yields Bi_2WO_6 as well as transient byproducts such as NH_3 and N_2O_5 (see Scheme 1A).[42,43]

In contrast, selecting precursors that yield non-transient byproducts via a metathesis reaction produces Bi_2WO_6 nanoplates (Figures 1C and 1D; sample USP-M Bi_2WO_6). Specifically, $BiCl_3$ and Na_2WO_4 were selected as precursors. In this case, when the precursor solution is prepared, colloidal BiOCl results from the hydrolysis of $BiCl_3$ (see Supporting Information, Figures S2A and S2B).[40] SEM of the dried precursor solution reveals no plate-like structures prior to USP (Supporting Information, Figure S2C). Thus, the overall pyrolysis process can be described by Scheme 1B, which is confirmed by thermal analysis of the precursor solution (see Figure 2 and Supporting Information, Figure S3). The nanoplates have an average diameter of 433 ± 134 nm and thickness of 46 ± 16 nm. The square symmetry of the ED (Figure 1D, inset) indicates that the nanoplates are single-crystalline and bound on the top and bottom

(41) Wang, W. N.; Purwanto, A.; Lenggoro, I. W.; Okuyama, K.; Chang, H.; Jang, H. D. *Ind. Eng. Chem. Res.* **2008**, *47*, 1650.

(42) Šulcová, P.; Trojan, M. *J. Therm. Anal. Calorim.* **2000**, *60*, 209.

(43) Bamford, C. H.; Tipper, C. F. H. *Reactions of Non-metallic Inorganic Compounds*; Elsevier: New York, 1972.

Scheme 2. Cross-Sectional Illustration of the Physical and Chemical Processes Occurring during the USP Synthesis of (A) Bi_2WO_6 Microspheres and (B) Bi_2WO_6 Nanoplates

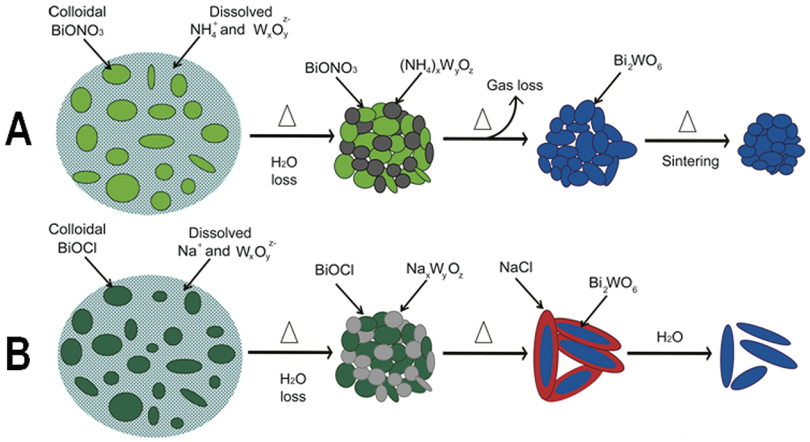

by {001} facets, consistent with their Aurivillius class crystal structure.[19,44]

The different particle structures can be correlated with the decomposition pathways of the various precursor combinations. To understand why both microspheres and nanoplates can be produced via USP, DSC and TGA of the dried precursor solutions were conducted. The results are shown in Figures 2A and 2B for the precursor combinations yielding USP Bi_2WO_6 and USP-M Bi_2WO_6, respectively. For USP Bi_2WO_6, no major endo- or exothermic processes are revealed by DSC. TGA shows several mass losses, with the first likely corresponding to adsorbed water and the subsequent losses to water of hydration and the volatile byproducts associated with nitrate and ammonium decomposition. On the basis of this information, Scheme 2A accounts for the formation of submicrometer, polycrystalline Bi_2WO_6 spheres from the $(NH_4)_{10}H_2(W_2O_7)_6$ and $Bi(NO_3)_3$-based precursor solution. As the aerosol droplets are heated, water is removed, resulting in dried particles composed of the precursors. The precursors then react in the solid state, forming Bi_2WO_6 particles and releasing gaseous byproducts. Once formed, the product particles continue to be heated, becoming more compact via sintering until they are collected outside the heated zone.

Mass losses associated with water are also revealed by TGA of the dried precursors yielding USP-M Bi_2WO_6. In contrast, DSC reveals a significant exothermic peak with an onset of 337 °C. This feature is characteristic of metathesis reactions in which stable salts such as NaCl are generated as a byproduct.[45,46] Indeed, NaCl formation was confirmed by EDS analysis and powder XRD of the unwashed product; washing removes NaCl from the plates (Supporting Information, Figure S3). On the basis of this information, Scheme 2B accounts for the formation of Bi_2WO_6 nanoplates by USP. Just as with USP Bi_2WO_6, water is first removed during heating. As the dried precursor particles continue through the heated zone, the solid state metathesis reaction is initiated (Scheme 1B). Bi_2WO_6 formation likely nucleates at multiple spots within a droplet, but the byproduct NaCl inhibits sintering between the formed crystals. This condition, coupled with the released heat from the metathesis reaction, facilitates their growth into larger particles, with the most thermodynamically favored facet expressed. Interestingly, the addition of surfactants and inert salts to precursor solutions has been reported to inhibit subparticle consolidation during aerosol processes;[47,48] however, the crystal habit of the resultant nanoparticles was not controlled to give particles with defined shapes.

Other precursor combinations are also capable of yielding Bi_2WO_6 and non-transient byproducts. For example, Li_2WO_4 and BiOCl, Na_2WO_4 and BiOBr (generated in situ from the hydrolysis of $BiBr_3$), and Li_2WO_4 and BiOBr can undergo metathesis at elevated temperatures. When coupled with USP, single-crystalline nanoplates were again synthesized, but the samples were not phase pure, with other particle structures also observed and arising from either unreacted starting material or secondary bismuth tungstate phases. Interestingly, high-quality Bi_2WO_6 nanoplates can also be prepared by USP from a starting solution of $Bi(NO_3)_3$ and Na_2WO_4. In this case, $NaNO_3$ is not collected as a byproduct as the nitrate ion decomposes during pyrolysis, but Na is detected by EDS analysis of the unwashed particles. These results suggest that the alkali cation may serve as a habit modifier, stabilizing the {001} facets toward nanoplate growth. These results also indicate that a wider range of precursors may be considered when designing future syntheses that couple metathesis reactions with USP.

Additional Characterization. USP Bi_2WO_6 and USP-M Bi_2WO_6 were further characterized and compared to Bi_2WO_6 made by solid state heating of the parent metal oxides (sample SS Bi_2WO_6) as well as the metathesis precursors (sample SS-M Bi_2WO_6). SEM images of SS Bi_2WO_6 and SS-M Bi_2WO_6 are shown in Supporting Information, Figure S4. Notably, the bulk sample prepared by heating

(44) Schaak, R. E.; Mallouk, T. E. *Chem. Mater.* **2002**, *14*, 1455.
(45) Brown, M. E. *Introduction to Thermal Analysis: Techniques and Applications*, 2nd ed.; Kluwer Academic Publishers: Norwell, MA, 2001.
(46) Gillan, E. G.; Kaner, R. B. *Chem. Mater.* **1996**, *8*, 333.
(47) Didenko, Y. T.; Suslick, K. S. *J. Am. Chem. Soc.* **2005**, *127*, 12196.
(48) Xia, B.; Lenggoro, I. W.; Okuyama, K. *Adv. Mater.* **2001**, *13*, 1579.

Table 1. Summary of BET Surface Areas

Sample	BET surface area (m^2/g)
SS Bi_2WO_6	< 1
SS-M Bi_2WO_6	< 1
USP Bi_2WO_6	4
USP-M Bi_2WO_6	7

of the metathesis precursors did not generate nanoplates. This observation indicates that the spatial and temporal confinements provided by the aerosol synthesis are also critical to nanoplate formation and could provide similar advantages when other metathesis processes are incorporated into USP. Total surface area measurements determined by BET analysis are listed in Table 1. The samples prepared by conventional solid state heating methods have very low surface areas (< 1 m^2/g) regardless of the starting precursors. Both samples prepared by USP have higher surface areas.

The XRD patterns of all samples were indexed to γ-Bi_2WO_6 (JCPDS 73-1126) (Figure 3). Comparatively broadened reflections were obtained from USP Bi_2WO_6, with an average crystallite size of 17 nm being calculated from the {131} reflection. This estimate is consistent with TEM of USP Bi_2WO_6. This same analysis for USP-M Bi_2WO_6 is unreliable given its nanoplate morphology. Yet, the sharper reflections indicate the formation of a more crystalline sample, which is facilitated by the release of heat from the metathesis reaction. On the basis of the crystal structure of Bi_2WO_6 and SEM analysis, the nanoplates are expected to consist of ~35−75 $\{Bi_2O_2^{2+}/WO_4^{2-}\}$ units.

The electronic states of Bi and W were determined by XPS for the various samples. Both USP Bi_2WO_6 and USP-M Bi_2WO_6 showed spin-coupled W($4f^{7/2}$, $4f^{5/2}$) and Bi($4f^{7/2}$, $4f^{5/2}$) doublets at the binding energies consistent with conventional Bi_2WO_6 (Figures 4a and 4b). However, differences emerged when analyzing the O 1s core-level of the various samples (Figure 4c). SS Bi_2WO_6, SS-M Bi_2WO_6, and USP-M Bi_2WO_6 displayed a narrow peak centered at

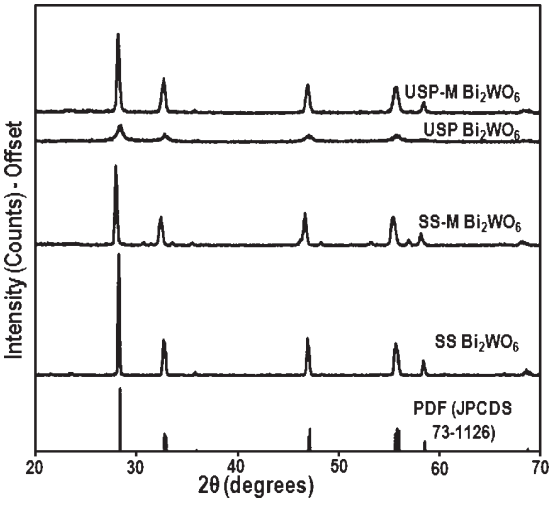

Figure 3. XRD powder patterns for USP-M Bi_2WO_6, USP Bi_2WO_6, SS-M Bi_2WO_6, and SS Bi_2WO_6. Included for reference is the PDF for γ-Bi_2WO_6 (JCPDS 73-1126).

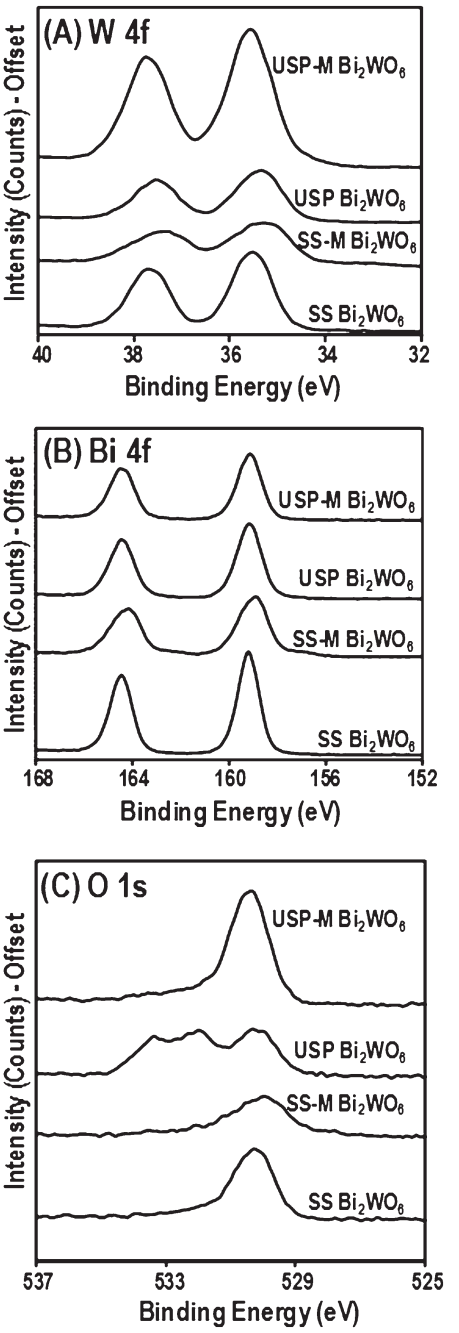

Figure 4. XPS analysis of USP-M Bi_2WO_6, USP Bi_2WO_6, SS-M Bi_2WO_6, and SS Bi_2WO_6. In (A), the W 4f region, in (B) the Bi 4f region, and in (C) the O 1s region.

a binding energy of ~530.5 eV, which is consistent with lattice W−O.[49] Slight tailing to higher binding energies was observed, which is ascribed to Bi−O.[49] In contrast, the O 1s region of USP Bi_2WO_6 consists of a broadened feature extending from 529 to 535 eV. This dramatic change in line shape indicates that multiple chemical environments exist for oxygen, with $M_{W,Bi}-OH_{ads}$ and H_2O_{ads} accounting for the broadening to higher binding energies.[50,51] The high

(49) Crist, B. V. *Handbook of Monochromatic XPS Spectra: The Elements and Native Oxides*; Wiley: Chichester, 2000.
(50) Dupin, J.-C.; Gonbeau, D.; Vinatier, P.; Levasseur, A. *Phys. Chem. Chem. Phys.* **2000**, *2*, 1319.

prevalence of hydroxyl groups and adsorbed water indicates that the USP Bi_2WO_6 sample is more hydrophilic than the other samples.[52,53]

Bulk elemental analysis and energy dispersive X-ray (EDX) analysis were consistent with the formation of stoichiometric Bi_2WO_6, but quantitative XPS revealed different surface Bi-to-W ratios. In fact, USP-M Bi_2WO_6 is substantially enriched with tungsten compared to the other samples ($Bi_{0.5}W$ for USP-M Bi_2WO_6 compared to $Bi_{1.75}W$, $Bi_{1.4}W$, $Bi_{1.75}W$ for USP Bi_2WO_6, SS Bi_2WO_6, and SS-M Bi_2WO_6, respectively), indicating that the nanoplates are terminated primarily by a $\{WO_4^{2-}\}$ layer. Interestingly, the survey scan for USP-M Bi_2WO_6 revealed trace sodium, Na^+ (Supporting Information, Figure S5). As Na^+ cannot substitute for Bi^{3+} in the Bi_2WO_6 crystal lattice,[19] it is confined to and stabilizes the negatively charged surfaces of the nanoplates, which is consistent with the results from ED, EDS, XRD, and elemental analysis and its proposed role as a habit modifier. As this comparative analysis reveals, in addition to modifying the particle structure, the integration of metathesis chemistry into spray pyrolysis can greatly alter the surface properties of the resultant particles.

Conclusions

The development of scalable synthetic routes to compositionally complex materials as samples with well-defined size, shape, composition, and crystal-phase is important for many applications and studies of fundamental structure−function relationships. Here, a metathesis reaction was coupled with USP for the first time. The non-transient byproduct and heat produced modified the crystal growth conditions, facilitating the formation of single-crystalline Bi_2WO_6 nanoplates, when microspheres are otherwise synthesized. Significantly, a range of solid-state metathesis reactions have been previously demonstrated, rapidly producing crystalline powders that are structurally ill-defined.[46] The spatial and temporal confinement achieved with this aerosol method provides a way of harnessing metathesis chemistry to produce single-crystalline shape-controlled particles and should be generally applicable to a host of compositionally complex solids. The main challenges lie in identifying additional precursor combinations that yield stable solutions suitable for integration into USP. Beyond the BiOCl colloids employed here, other suitable metal oxyhalide phases are known (e.g., SbOCl and LnOCl's where Ln = La, Sm, and Gd) while other solvent systems and spray techniques may be applicable.[54] Generally speaking, the integration of new chemical methods into USP that yield non-transient byproducts represents a promising means of achieving structurally diverse particles.

Acknowledgment. We acknowledge financial support from Indiana University, ACS-PRF 48790-DNI10, and NSF CAREER DMR-0955028. XPS analysis was carried out in the Frederick Seitz Materials Research Laboratory Central Facilities, University of Illinois, which are partially supported by the U.S. Department of Energy under Grants DE-FG02-07ER46453 and DE-FG02-07ER46471. The authors would also like to thank Dr. Maren Pink of the Indiana University Molecular Structure Center, Dr. David G. Morgan of the Indiana University Nanoscale Characterization Facility, Dr. Ellen Steinmiller, and Susanne Wicker for their valuable advice as well as Rudiger Laufhutte at the Microanalysis Laboratory for assistance with elemental analysis and Rick Haasch for assistance with XPS in the Center for Microanalysis of Materials, both at the University of Illinois at Urbana−Champaign.

Supporting Information Available: A schematic of the USP setup as well as characterization of the USP-M Bi_2WO_6 precursor solution and unwashed USP-M Bi_2WO_6 product are provided. SEM images of SS Bi_2WO_6 and SS-M Bi_2WO_6 are also included. This material is available free of charge via the Internet at http://pubs.acs.org.

(51) Dharmadhikari, V. S.; Sainkar, S. R.; Badrinarayan, S.; Goswami, A. *J. Electron Spectrosc. Relat. Phenom.* **1982**, *25*, 181.
(52) Nakamura, M.; Sirghi, L.; Aoki, T.; Hatanaka, Y. *Surf. Sci.* **2002**, *507−510*, 778.
(53) Salmeron, M.; Bluhm, H.; Tatarkhanov, M.; Ketteler, G.; Shimizu, T. K.; Mugarza, A.; Deng, X.; Herranz, T.; Yamamoto, S.; Nilsson, A. *Faraday Discuss.* **2009**, *141*, 221.
(54) Perera, S.; Zelenski, N. A.; Pho, R. E.; Gillan, E. G. *J. Solid State Chem.* **2007**, *180*, 2916.